



DØnote 5487-CONF

Version 1.1

Send comments to d0-run2eb-004@fnal.gov & d0-run2eb-005@fnal.gov
by Aug 17, noon (FNAL time)

Author(s): Gregorio Bernardi & Wade Fisher for the Higgs Group

Combined Upper Limits on Standard Model Higgs Boson Production from the DØ Experiment in 0.9-1.7 fb⁻¹

The DØ Collaboration
URL <http://www-d0.fnal.gov>
(Dated: August 16, 2007)

Upper limits on the cross section for standard model Higgs-boson production in $p\bar{p} \rightarrow H + X$ at $\sqrt{s} = 1.96$ TeV are determined for $105 < m_H < 200$ GeV/c². The contributing production processes include associated production ($WH \rightarrow \ell\nu b\bar{b}$, $ZH \rightarrow \ell\ell/\nu\nu b\bar{b}$, $WH \rightarrow WW^+W^-$) and gluon fusion ($H \rightarrow W^+W^-$). Analyses are conducted with integrated luminosities from 0.9 fb⁻¹ to 1.7 fb⁻¹ recorded by the DØ experiment. The results are in good agreement with background expectations and the observed 95% C.L. upper limits are found to be a factor of 8.3 (3.5) higher than the standard model cross section at $m_H = 115$ (160) GeV/c² while the expected limits are found to be 6.0 (4.6) for the same masses.

Preliminary Results for Summer 2007 Conferences

TABLE I: List of analysis channels, corresponding integrated luminosities, and final variables. See the Introduction for details. The final variable used for several analyses is a neural-network discriminant output which is abbreviated as NN discriminant.

Channel	Luminosity (fb^{-1})	Final Variable	Reference
$WH \rightarrow e\nu b\bar{b}$ RunIIa, ST/DT	1.04	NN discriminant	[4]
$WH \rightarrow e\nu b\bar{b}$ RunIIb, ST/DT	0.64	NN discriminant	[4]
$WH \rightarrow \mu\nu b\bar{b}$ RunIIa, ST/DT	1.05	NN discriminant	[4]
$WH \rightarrow \mu\nu b\bar{b}$ RunIIb, ST/DT	0.63	NN discriminant	[4]
$WH \rightarrow \ell\nu b\bar{b}$ RunIIa, DT	0.93	Dijet mass	[5]
$ZH \rightarrow \nu\bar{\nu} b\bar{b}$ RunIIa, DT	0.93	Dijet mass	[5]
$ZH \rightarrow \mu^+\mu^- b\bar{b}$ RunIIa, ST/DT	1.10	NN discriminant	[6]
$ZH \rightarrow e^+e^- b\bar{b}$ RunIIa, ST/DT	1.10	NN discriminant	[6]
$WH \rightarrow WW^+W^- (e^\pm e^\pm)$ RunIIa	1.00	2-D Likelihood	[7]
$WH \rightarrow WW^+W^- (e^\pm \mu^\pm)$ RunIIa	1.00	2-D Likelihood	[7]
$WH \rightarrow WW^+W^- (\mu^\pm \mu^\pm)$ RunIIa	1.00	2-D Likelihood	[7]
$H \rightarrow W^+W^- (e^+e^-)$ RunIIa	0.95	$\Delta\varphi(e^+, e^-)$	[8]
$H \rightarrow W^+W^- (e^\pm \mu^\mp)$ RunIIa	0.95	$\Delta\varphi(e^\pm, \mu^\mp)$	[8]
$H \rightarrow W^+W^- (\mu^+\mu^-)$ RunIIa	0.95	$\Delta\varphi(\mu^+, \mu^-)$	[9]
$H \rightarrow W^+W^- (e^\pm \mu^\mp)$ RunIIb	0.64	NN discriminant	[10]

I. INTRODUCTION

Despite its success as a predictive tool, the standard model (SM) of particle physics remains incomplete without a means to explain electroweak-symmetry breaking. The simplest proposed mechanism involves the introduction of a complex doublet of scalar fields that generate particle masses via their mutual interactions. After accounting for longitudinal polarizations for the electroweak bosons, this so-called Higgs mechanism also gives rise to a single scalar boson with an unpredicted mass. Direct searches in $e^+e^- \rightarrow Z^* \rightarrow ZH$ at the Large Electron Positron (LEP) collider yielded lower mass limits at $m_H > 114.4 \text{ GeV}/c^2$ [1] while indirect constraints favor $m_H < 182 \text{ GeV}/c^2$ [2], with both limits set at 95% C.L. The SM Higgs-boson search is one of the main goals of the Fermilab Tevatron physics program.

In this note, we combine recent results for direct searches for SM Higgs bosons in $p\bar{p}$ collisions at $\sqrt{s} = 1.96 \text{ TeV}$ and recorded by the DØ experiment [3]. These are searches for Higgs bosons produced in association with vector bosons ($p\bar{p} \rightarrow W/ZH \rightarrow \ell\nu/\ell\ell/\nu\nu b\bar{b}$ and $p\bar{p} \rightarrow WH \rightarrow WW^+W^-$) or singly through gluon-gluon fusion ($p\bar{p} \rightarrow H \rightarrow W^+W^-$). The searches were conducted with data collected during the period 2002-2007 and correspond to integrated luminosities ranging from 0.9 fb^{-1} to 1.7 fb^{-1} . The searches are organized into fifteen final states, each designed to isolate a particular Higgs-boson production and decay mode. In order to ensure proper combination of signals, the analyses were designed to be mutually exclusive after analysis selections. Searches for several final states are performed in two distinct epochs of data collection: before and after the 2006 DZero detector upgrade. The two epochs are denoted as RunIIa and RunIIb. This results in a total of twenty-one individual analyses.

The twenty-one analyses [4–10] are outlined in Table I. In the cases of $p\bar{p} \rightarrow W/ZH$ production, we search for a Higgs-boson decaying to two bottom-quarks. The decays of the vector bosons further define the analyzed final states: $WH \rightarrow \ell\nu b\bar{b}$, $ZH \rightarrow \ell\ell b\bar{b}$, $ZH \rightarrow \nu\bar{\nu} b\bar{b}$. For the $WH \rightarrow \ell\nu b\bar{b}$, and $ZH \rightarrow \ell\ell b\bar{b}$ decays, the analyses are separated into two orthogonal groups: one in which two of the jets were b -tagged (herein called double-tag or DT) and one group in which only one jet was tagged (single-tag or ST). For these analyses, only final states with exactly two jets are selected. For the $ZH \rightarrow \nu\bar{\nu} b\bar{b}$ analysis, only an asymmetric double-tag is considered and two or more jets are required in the final state. In the case of $WH \rightarrow \ell\nu b\bar{b}$ production, the primary lepton from the W -boson decay may fall outside of the detector fiducial volume or is not reconstructible. This case is treated as a separate WH analysis, to which we refer as $WH \rightarrow \ell\nu b\bar{b}$. For this channel, the background is the same as the $ZH \rightarrow \nu\bar{\nu} b\bar{b}$ analysis.

We also consider Higgs decays to two W^\pm bosons. For $WH \rightarrow WW^+W^-$ production, we search for leptonic W -boson decays with three final states of same-signed leptons: $WWW \rightarrow e^\pm \nu e^\pm \nu + X$, $e^\pm \nu \mu^\pm \nu + X$, and $\mu^\pm \nu \mu^\pm \nu + X$. In the case of $p\bar{p} \rightarrow H \rightarrow W^+W^-$ production, we search for leptonic W boson decays with three final states of opposite-signed leptons: $WW \rightarrow e^+ \nu e^- \nu$, $e^\pm \nu \mu^\mp \nu$, and $\mu^+ \nu \mu^- \nu$. For the gluon fusion process, $H \rightarrow b\bar{b}$ decays are not considered due to the large multijets background.

All Higgs signals are simulated using PYTHIA v6.202 [11] using CTEQ6L1 [12] leading order parton distribution functions. The signal cross sections are normalized to next-to-next-to-leading order (NNLO) calculations [13, 14] and branching ratios are calculated using HDECAY [15]. The contributions from multijet backgrounds (QCD production) are measured in data. The other backgrounds were generated by PYTHIA, ALPGEN [16], and COMPHEP [17], with PYTHIA providing parton-showering and hadronization. Background cross sections are either normalized to

next-to-leading order (NLO) calculations from MCFM [18] or to data control samples.

II. LIMIT CALCULATIONS

We combine results using the CL_s method with a log-likelihood ratio (LLR) test statistic [19]. The value of CL_s is defined as $CL_s = CL_{s+b}/CL_b$ where CL_{s+b} and CL_b are the confidence levels for the signal-plus-background hypothesis and the background-only hypothesis, respectively. These confidence levels are evaluated by integrating corresponding LLR distributions populated by simulating outcomes via Poisson statistics. Separate channels and bins are combined by summing LLR values over all bins and channels. This method provides a robust means of combining individual channels while maintaining individual channel sensitivities and incorporating systematic uncertainties. Systematics are treated as uncertainties on the expected numbers of signal and background events, not the outcomes of the limit calculations. This approach ensures that the uncertainties and their correlations are propagated to the outcome with their proper weights. The CL_s approach used in this analysis utilizes binned final-variable distributions rather than a single-bin (fully integrated) value for each contributing analysis.

A. Final Variable Preparation

For the $WH \rightarrow \ell\nu b\bar{b}$ and $ZH \rightarrow \ell\ell b\bar{b}$ analyses, the final variable used for limit setting is the output of a neural-network (NN) discriminant, trained separately for each Higgs mass tested. The $ZH \rightarrow \nu\bar{\nu} b\bar{b}$ and $WH \rightarrow \ell\nu b\bar{b}$ analyses use the invariant dijet mass as a final variable. In the $H \rightarrow W^+W^-$ analyses, the Higgs mass cannot be directly reconstructed due to the neutrinos in the final state. Therefore, the RunIIa $p\bar{p} \rightarrow H \rightarrow W^+W^-$ analyses use the difference in the azimuthal angle (φ) between the two final state leptons ($\Delta\varphi(\ell_1, \ell_2)$). The RunIIb $p\bar{p} \rightarrow H \rightarrow W^+W^-$ analysis uses a NN discriminant trained for each Higgs mass tested. The $WH \rightarrow WW^+W^-$ analysis utilizes a two-dimensional likelihood discriminant as a final variable. Each background final variable is smoothed via Gaussian kernel estimation [20] to minimize any statistical fluctuation in the shape of the final variable. Examples of these types of distributions are shown in Figs. 1a-d and Figs. 2a-d.

To decrease the granularity of the steps between simulated Higgs masses in the limit calculation, additional Higgs mass points are created via signal point interpolation [21]. The primary motivation of this procedure is to provide a means of combining analyses which do not share a common simulated Higgs mass. However, this procedure also allows a measurement of the behavior of each limit on a finer granularity than otherwise possible.

B. Systematic Uncertainties

The systematic uncertainties differ between analyses for both the signals and backgrounds [4–10]. Here we will summarize only the largest contributions. All analyses carry an uncertainty on the integrated luminosity of 6.1%. The $H \rightarrow b\bar{b}$ analyses have an uncertainty on the b -tagging rate of 4-6% per tagged jet. These analyses also have an uncertainty on the jet measurement and acceptances of $\sim 7.5\%$. For the $H \rightarrow W^+W^-$ analyses, the largest uncertainties are those associated with lepton measurement and acceptances. These values range from 3-6% depending on the final state. The largest contribution for all analyses is the uncertainty on the background cross sections at 6-18% depending on the background. The uncertainty on the expected multijet background is dominated by the statistics of the data sample from which it is estimated, and is considered separately from the other cross section uncertainties. The $p\bar{p} \rightarrow H \rightarrow W^+W^-$ analyses are also assigned a 10% uncertainty on the NNLO Higgs production cross section associated with the accuracy of the theoretical calculation. Further details on the systematic uncertainties are given in Table II.

The systematic uncertainties for the background rates are generally several times larger than the signal expectation itself and are thus an important factor in the calculation of limits. As such, each systematic uncertainty is folded into the signal and background expectations in the limit calculation via Gaussian distribution. These Gaussian values are sampled for each Poisson trial (pseudo-experiment). Correlations between systematic sources are carried through in the calculation. For example, the uncertainty on the integrated luminosity is held to be correlated between all signals and backgrounds and, thus, the same fluctuation in the luminosity is common to all channels for a single pseudo-experiment. All systematic uncertainties originating from a common source are held to be correlated, as detailed in Tables II and III.

To minimize the degrading effects of systematics on the search sensitivity, the individual background contributions are fitted to the data observation by minimizing a profile likelihood function [22]. The fit computes the optimal central values for the systematic uncertainties, while accounting for departures from the nominal predictions. A fit is

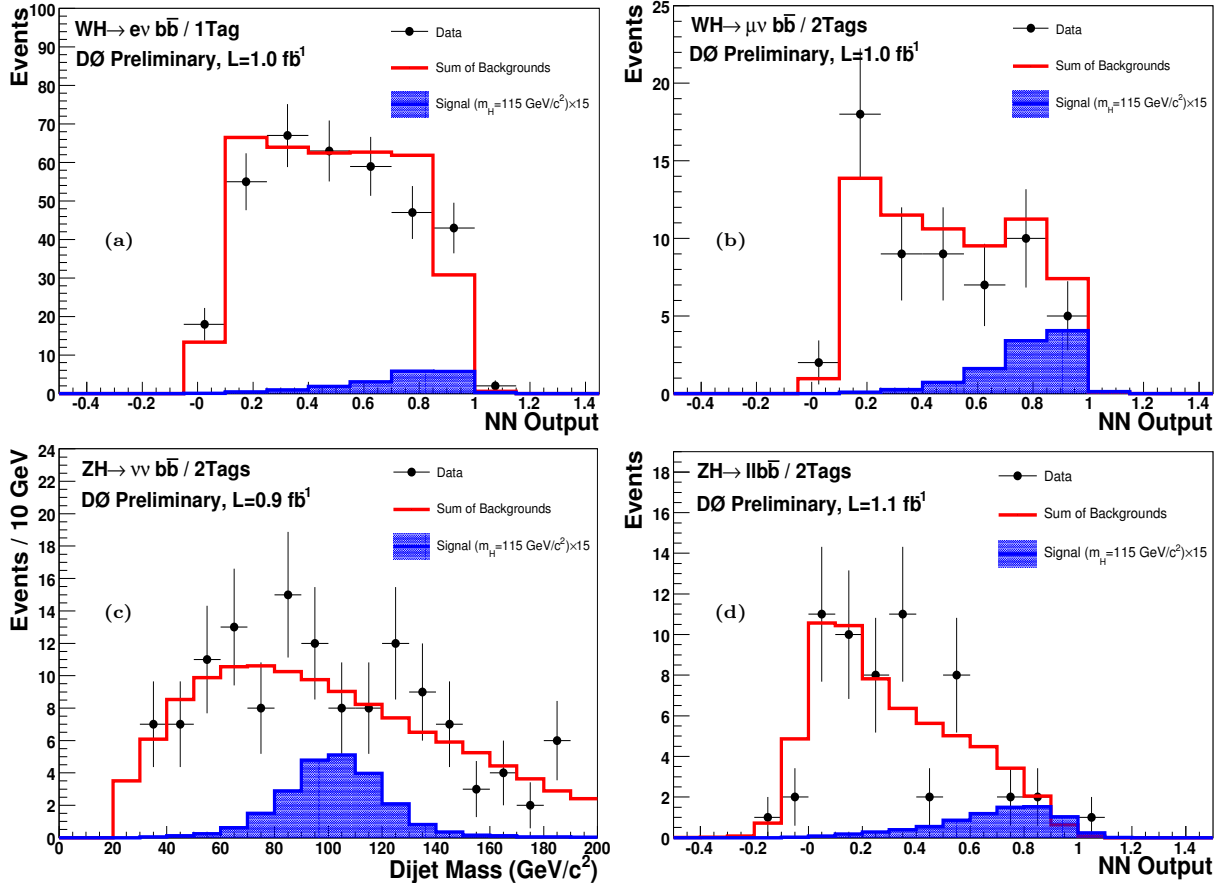


FIG. 1: Final variable distributions for selected Higgs search analyses. The figure contains distributions for: the NN discriminant for the $WH \rightarrow e\nu b\bar{b}$ ST analysis (a), the NN discriminant for the $WH \rightarrow \mu\nu b\bar{b}$ DT analysis (b), the dijet invariant mass for the $ZH \rightarrow \nu\nu b\bar{b}$ DT analysis (ZH signal only)(c), the neural-network discriminant for the $ZH \rightarrow \ell\ell b\bar{b}$ DT analyses (d). For each figure, the total background expectations and observed data are shown. The expected Higgs signals at selected masses are scaled as indicated.

performed to the background-only hypothesis separately for each Poisson MC trial, and is constrained to bins with signal expectations less than 4% of the total expected background. To ensure a reliable implementation, additional coverage studies are performed to ensure the accuracy of the calculation.

III. DERIVED UPPER LIMITS

We derive limits on SM Higgs-boson production $\sigma \times BR(H \rightarrow b\bar{b}/W^+W^-)$ via twenty-one individual analyses [4–10]. The limits are derived at a 95% C.L. To facilitate model transparency and to accommodate analyses with different degrees of sensitivity, we present our results in terms of the ratio of 95% C.L. upper cross section limits to the SM cross section as a function of Higgs mass. The SM prediction for Higgs-boson production would therefore be considered excluded at 95% C.L. when this limit ratio falls below unity. For the combined limit, the $WH \rightarrow \ell\nu b\bar{b}$ and $ZH \rightarrow \nu\nu b\bar{b}$ signals are summed and their common background only enters the calculation once.

The individual analyses described above are grouped to evaluate combined limits over the range $105 \leq m_H \leq 200 \text{ GeV}/c^2$. The $WH \rightarrow \ell\nu b\bar{b}$ and $ZH \rightarrow \ell\ell/\nu\nu b\bar{b}$ analyses contribute to the region $m_H \leq 140 \text{ GeV}/c^2$, while the $H \rightarrow W^+W^-$ and $WH \rightarrow WW^+W^-$ analyses contribute for $m_H \geq 120 \text{ GeV}/c^2$.

Figure 3 shows the expected and observed 95% C.L. cross section limit ratios for all analyses combined in the low- and high-mass regions ($105 \leq m_H \leq 200 \text{ GeV}/c^2$). The LLR distributions for the full combination are shown in Fig. 4. Included in these figures are the LLR values for the signal-plus-background hypothesis (LLR_{s+b}), background-only hypothesis (LLR_b), and the observed data (LLR_{obs}). The shaded bands represent the 1 and 2 standard deviation (σ) departures for LLR_b . These distributions can be interpreted as follows:

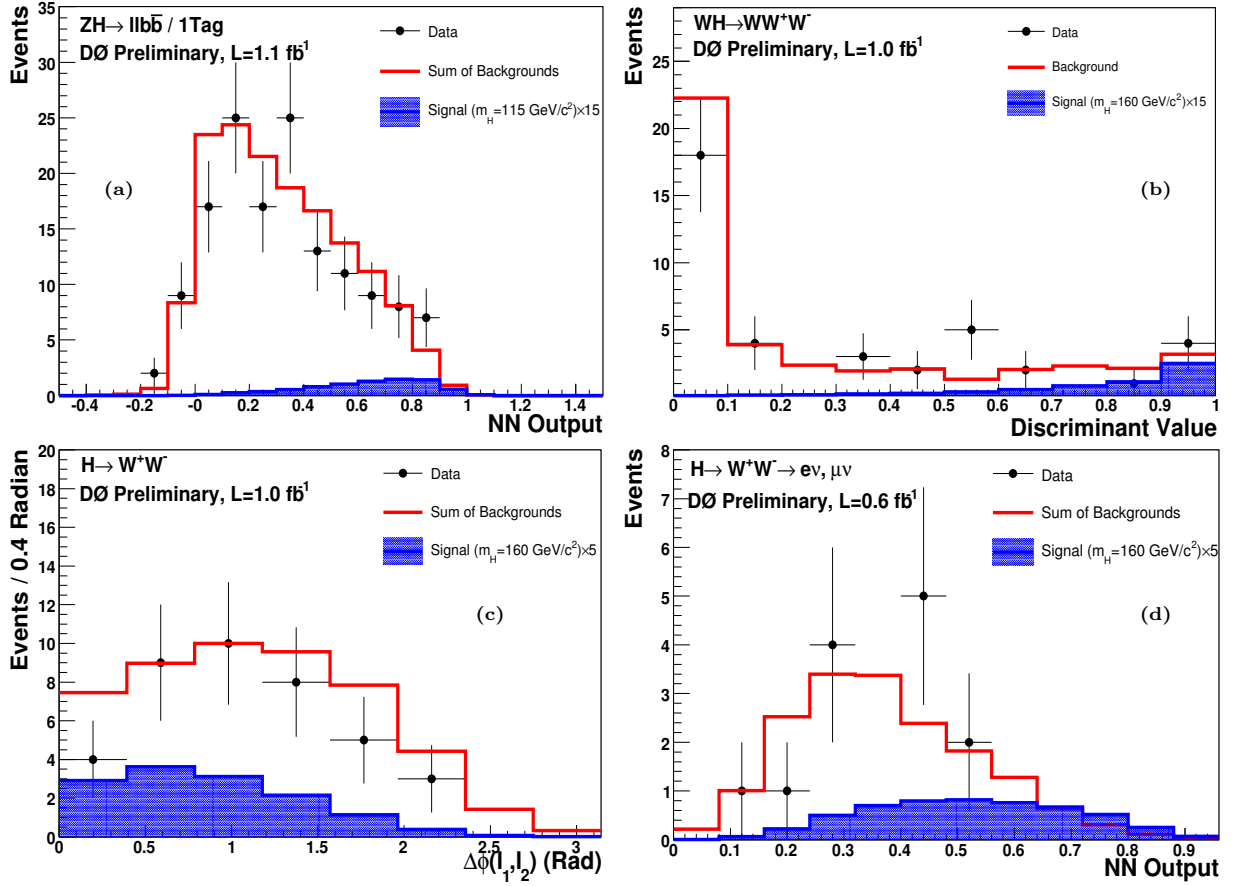


FIG. 2: Final variable distributions for selected Higgs search analyses. The figure contains distributions for: the NN discriminant for the $ZH \rightarrow \ell\ell b\bar{b}$ ST analysis (a), a one-dimensional projection of the two-dimensional likelihood for the $WH \rightarrow WW^+W^-$ analyses (b), $\Delta\varphi(\ell_1, \ell_2)$ for the RunIIa $H \rightarrow W^+W^-$ analyses (c), the neural-network discriminant for the RunIIb hww analysis (d). For each figure, the total background expectations and observed data are shown. The expected Higgs signals at selected masses are scaled as indicated.

- The separation between LLR_b and LLR_{s+b} provides a measure of the discriminating power of the search. This is the ability of the analysis to separate the $s + b$ and b -only hypotheses.
- The width of the LLR_b distribution (shown here as one and two standard deviation (σ) bands) provides an estimate of how sensitive the analysis is to a signal-like fluctuation in data, taking account of the presence of systematic uncertainties. For example, when a $1\text{-}\sigma$ background fluctuation is large compared to the signal expectation, the analysis sensitivity is thereby limited.
- The value of LLR_{obs} relative to LLR_{s+b} and LLR_b indicates whether the data distribution appears to be more signal-like or background-like. As noted above, the significance of any departures of LLR_{obs} from LLR_b can be evaluated by the width of the LLR_b distribution.

IV. CONCLUSIONS

We have presented results for eleven Higgs search analyses. We have combined these analyses and form new limits more sensitive than each individual limit. The observed (expected) 95% C.L. limit ratios to SM cross sections on $p\bar{p} \rightarrow WH/ZH/H, H \rightarrow b\bar{b}/W^+W^-$ range from 8.3 (6.0) at $m_H = 115 \text{ GeV}/c^2$ and 3.5 (4.6) at $m_H = 160 \text{ GeV}/c^2$.

TABLE II: List of leading correlated systematic uncertainties. The values for the systematic uncertainties are the same for the $ZH \rightarrow \nu\bar{\nu}b\bar{b}$ and $WH \rightarrow \ell\nu b\bar{b}$ channels. All uncertainties within a group are considered 100% correlated across channels. The correlated systematic uncertainty on the background cross section (σ) is itself subdivided according to the different background processes in each analysis.

Source	$WH \rightarrow e\nu b\bar{b}$ DT(ST)	$WH \rightarrow \mu\nu b\bar{b}$ DT(ST)	$WH \rightarrow WW^+W^-$	$H \rightarrow W^+W^-$
Luminosity (%)	6.1	6.1	0	0
Normalization (%)	0	0	6.1	6.1
Jet Energy Scale (%)	3.0	3.0	0	3.0
Jet ID (%)	3.0	3.0	0	0
Electron ID/Trigger (%)	6.0	0	11	2.3-10
Muon ID/Trigger (%)	0	11.0	11	7.7-10
b -Jet Tagging (%)	9.2(4.6)	9.2(4.6)	0	0
Background σ (%)	6-18	6-18	6-18	6-18

Source	$ZH \rightarrow \nu\bar{\nu}b\bar{b}$	$ZH \rightarrow e^+e^-b\bar{b}$ DT(ST)	$ZH \rightarrow \mu^+\mu^-b\bar{b}$ DT(ST)
Luminosity (%)	6.1	6.1	0
Normalization (%)	0	0	6.1
Jet Energy Scale (%)	5.0	2.0	2.0
Jet ID (%)	7.1	5.0	5.0
Electron ID/Trigger (%)	0	4.0	0
Muon ID/Trigger (%)	0	0	4.0
b -Jet Tagging (%)	9.6	7.5(3.0)	7.5.0(3.0)
Background σ (%)	6-18	6-18	6-18

TABLE III: The correlation matrix for the analysis channels. The correlations for the $ZH \rightarrow \nu\bar{\nu}b\bar{b}$ and $WH \rightarrow \ell\nu b\bar{b}$ channels are held to be the same. All uncertainties within a group are considered 100% correlated across channels. The correlated systematic uncertainty on the background cross section (σ) is itself subdivided according to the different background processes in each analysis.

Source	$WH \rightarrow e\nu b\bar{b}$	$WH \rightarrow \mu\nu b\bar{b}$	$ZH \rightarrow \nu\bar{\nu}b\bar{b}$	$ZH \rightarrow \ell\ell b\bar{b}$	$H \rightarrow W^+W^-$	$WH \rightarrow WW^+W^-$
Luminosity	×	×	×	×		
Normalization				×	×	×
Jet Energy Scale	×	×	×	×	×	
Jet ID	×	×	×	×		
Electron ID/Trigger	×			×	×	×
Muon ID/Trigger		×		×	×	×
b -Jet Tagging	×	×	×	×		
Background σ	×	×	×	×	×	×

Acknowledgments

We thank the staffs at Fermilab and collaborating institutions, and acknowledge support from the DOE and NSF (USA); CEA and CNRS/IN2P3 (France); FASI, Rosatom and RFBR (Russia); CAPES, CNPq, FAPERJ, FAPESP and FUNDUNESP (Brazil); DAE and DST (India); Colciencias (Colombia); CONACyT (Mexico); KRF and KOSEF (Korea); CONICET and UBACyT (Argentina); FOM (The Netherlands); PPARC (United Kingdom); MSMT (Czech Republic); CRC Program, CFI, NSERC and WestGrid Project (Canada); BMBF and DFG (Germany); SFI (Ireland);

TABLE IV: Combined 95% C.L. limits on $\sigma \times BR(H \rightarrow b\bar{b}/W^+W^-)$ for SM Higgs-boson production. The limits are reported in units of the SM production cross section times branching fraction.

m_H (GeV/ c^2)	105	115	125	140	160	180	200
Expected	5.0	6.0	8.2	7.4	4.6	6.8	14.1
Observed	5.8	8.3	12.4	10.4	3.5	4.8	9.8

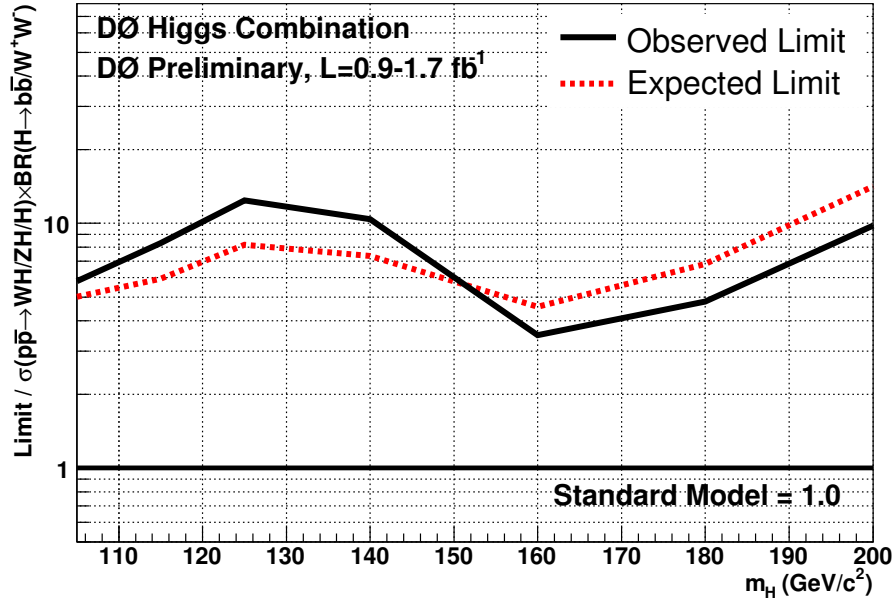


FIG. 3: Expected (median) and observed 95% C.L. cross section ratios for the combined $WH/ZH/H, H \rightarrow b\bar{b}/W^+W^-$ analyses over the $105 \leq m_H \leq 200$ GeV/c^2 mass range.

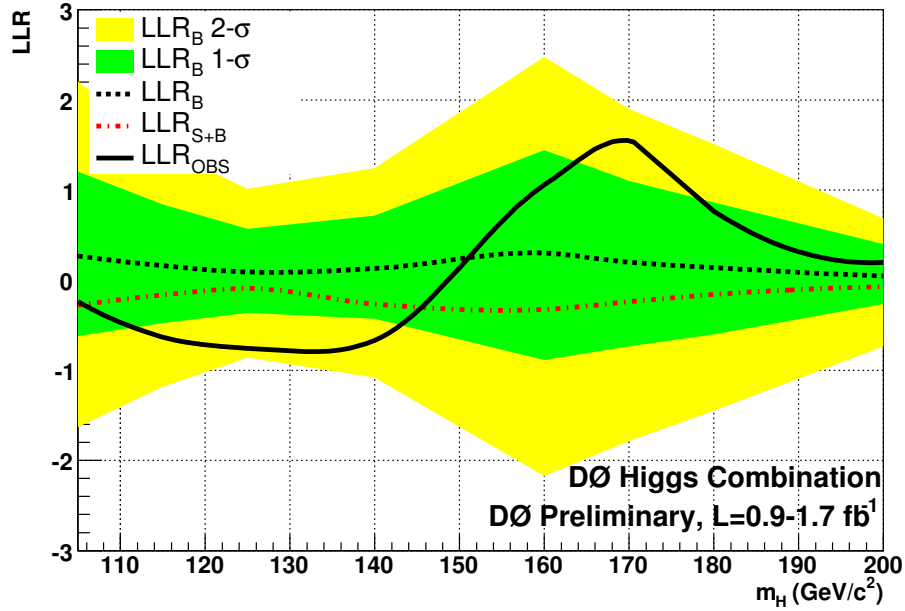


FIG. 4: Log-likelihood ratio distribution for the combined $WH/ZH/H, H \rightarrow b\bar{b}/W^+W^-$ analyses over the $105 \leq m_H \leq 200$ GeV/c^2 mass range.

Research Corporation, Alexander von Humboldt Foundation, and the Marie Curie Program.

-
- [1] R. Barate *et al.* [LEP Working Group for Higgs boson searches], Phys. Lett. B **565**, 61 (2003), [arXiv:hep-ex/0306033].
 - [2] LEP Electroweak Working Group: <http://lepewwg.web.cern.ch/LEPEWWG/> (March 2007 update <http://lepewwg.web.cern.ch/LEPEWWG/plots/winter2007/>).
 - [3] DØ Collaboration, V. Abazov *et. al.*, “The Upgraded DØ Detector”, Nucl. Instrum. Meth. A **565**, 463 (2006), [arXiv:hep-

- ex/0507191].
- [4] DØ Collaboration, “Search for WH Production using Neural Net Selection in $p\bar{p}$ Collisions at $\sqrt{s} = 1.96$ TeV with 1.7 fb^{-1} of Data,” DØ Conference Note 5472.
 - [5] DØ Collaboration, “A Search for Standard Model Higgs Boson in the Channel $ZH \rightarrow \nu\bar{\nu}b\bar{b}$ at $\sqrt{s} = 1.96$ TeV at DØ,” DØ Conference Note 5353.
 - [6] DØ Collaboration, “Search for $ZH(\rightarrow \ell^+\ell^-\bar{b}b)$ in $p\bar{p}$ collisions at $\sqrt{s} = 1960$ GeV,” DØ Conference Note 5482.
 - [7] DØ Collaboration, “Search for the Associated Higgs Boson Production $p\bar{p} \rightarrow WH \rightarrow WWW^* \rightarrow \ell^\pm \nu \ell'^\pm \nu' + X$ at $\sqrt{s} = 1.96$ TeV,” DØ Conference Note 5485.
 - [8] DØ Collaboration, “Search for the Higgs boson in $H \rightarrow WW^* \rightarrow l^+l^-(ee, e\mu)$ decays with 950 pb^{-1} at DØ in Run II,” DØ Conference Note 5063.
 - [9] DØ Collaboration, “Search for the Higgs boson in $H \rightarrow WW^* \rightarrow \mu\mu$ decays with 930 pb^{-1} at DØ in Run II,” DØ Conference Note 5194.
 - [10] DØ Collaboration, “Search for the Higgs boson in $H \rightarrow WW^* \rightarrow e\mu$ decays at DØ in Run IIB,” DØ Conference Note 5489.
 - [11] T. Sjöstrand, P. Edén, C. Friberg, L. Lönnblad, G. Miu, S. Mrenna and E. Norrbin, *Computer Phys. Commun.* **135** (2001) 238 (LU TP 00-30, [arXiv:hep-ph/0010017]).
 - [12] J. Pumplin *et al.*, “New Generation of Parton Distributions with Uncertainties from Global QCD Analysis”, *JHEP* 0207(2002)012 doi:10.1088/1126-6708/2002/07/012.
 - [13] S. Catani *et al.*, “Soft-gluon resummation for Higgs boson production at hadron colliders,” *JHEP* **0307**, 028 (2003), [arXiv:hep-ph/0306211].
 - [14] K. A. Assamagan *et al.* [Higgs Working Group Collaboration], “The Higgs working group: Summary report 2003,” [arXiv:hep-ph/0406152].
 - [15] A. Djouadi, J. Kalinowski and M. Spira, “HDECAY: A program for Higgs boson decays in the standard model and its supersymmetric extension,” *Comput. Phys. Commun.* **108**, 56 (1998) [arXiv:hep-ph/9704448].
 - [16] M. L. Mangano *et al.*, “ALPGEN, a generator for hard multiparton processes in hadronic collisions,” *JHEP* **0307**, 001 (2003) [arXiv:hep-ph/0206293].
 - [17] A. Pukhov *et al.*, “CompHEP: A package for evaluation of Feynman diagrams and integration over multi-particle phase space. User’s manual for version 33,” [arXiv:hep-ph/9908288].
 - [18] J. Campbell and R. K. Ellis, “Next-to-leading order corrections to $W + 2\text{jet}$ and $Z + 2\text{jet}$ production at hadron colliders,” *Phys. Rev. D* **65**, 113007 (2002), [arXiv:hep-ph/0202176].
 - [19] T. Junk, *Nucl. Instrum. Meth. A* **434**, 435-443 (1999). Alex Read, “Modified Frequentist Analysis of Search Results (The CLs Method)” CERN 2000-005 (30 May 2000).
 - [20] K. S. Cranmer, *Comput. Phys. Commun.*, **136**, 198 (2001), [arXiv:hep-ph/0011057].
 - [21] A. Read, *NIM A* 425 357-360 (1999).
 - [22] W. Fisher, “Systematics and Limit Calculations,” FERMILAB-TM-2386-E.
 - [23] CDF and DØ Collaborations, “Combined DØ and CDF Upper Limits on Standard-Model Higgs-Boson Production,” CDF Note 8384, DØ Note 5227.